Icarus 197 (2008) 549–555

Contents lists available at ScienceDirect

Icarus

www.elsevier.com/locate/icarus

Observation of a tilt of Titan's middle-atmospheric superrotation

Richard K. Achterberg [a,*], Barney J. Conrath [b], Peter J. Gierasch [b], F. Michael Flasar [c], Conor A. Nixon [a]

[a] University of Maryland, Department of Astronomy, College Park, MD 20742, USA
[b] Department of Astronomy, Cornell University, Ithaca, NY 14853, USA
[c] NASA Goddard Space Flight Center, Greenbelt, MD 20771, USA

ARTICLE INFO

Article history:
Received 11 December 2007
Revised 11 April 2008
Available online 5 June 2008

Keywords:
Titan
Atmospheres, structure
Atmospheres, dynamics
Infrared observations

ABSTRACT

Maps of isotherms on surfaces of constant pressure in Titan's middle atmosphere encircle the poles but show an offset, implying that the mean zonal flow has an axis of symmetry that is tilted relative to the spin axis of the solid body. The effect is seen in both hemispheres around a consistent axis. Periodogram analysis of the temperature field shows that wavenumber one, the signal corresponding to the spin tilt, is the strongest wave component. We conjecture that the tilt of the atmospheric spin is due to a feedback between the flow and the solar heating. The spin adjusts itself to align the spin equator with the direction toward the Sun, and thereby maximizes the efficiency with which the meridional circulation pumps angular momentum upward to generate superrotation.

1. Introduction

Observational evidence from several sources suggests that Titan's stratosphere rotates substantially more rapidly than the solid body of the satellite, which is approximately phase locked to Saturn with a rotational period of about 16 days (Stiles et al., 2008). Stratospheric temperature retrievals obtained from Voyager IRIS measurements near northern spring equinox imply latitudinal pressure gradients sufficiently large to require rapid atmospheric rotation, with the resulting centrifugal acceleration providing the necessary dynamical balance (Flasar et al., 1981; Flasar and Conrath, 1990). Doppler heterodyne spectroscopy measurements (Fast et al., 1994; Kostiuk et al., 2001, 2005) and stellar occultation central flash measurements (Hubbard et al., 1993; Sicardy et al., 1999; Bouchez, 2003) also support this conclusion. This aspect of Titan's atmospheric dynamics appears to be qualitatively similar to the atmospheric superrotation observed on Venus. However, the small tilt of Venus' spin axis (2.7°) to its orbital plane normal precludes strong seasonal effects, while Titan's larger tilt (26.7°) relative to Saturn's orbital plane, combined with a relatively short stratospheric radiative relaxation time, suggests possible significant seasonal modulation of its stratospheric spin. Observations of the response of Titan's atmosphere to seasonal variations in insolation can potentially provide new insight into the dynamics of super-rotating atmospheres. In this study, new evidence for tilt of atmospheric spin on Titan relative to the solid body is presented.

The Cassini orbiter Composite Infrared Spectrometer (CIRS) is currently acquiring a large body of new measurements of Titan's atmospheric thermal structure. Thermal mapping began in July 2004 and continues at the present time. Both limb and nadir viewing measurements have been made, with the former giving extensive spatial coverage of the middle stratosphere, and the later extending the temperature retrievals to higher altitudes, but with limited spatial coverage. A preliminary analysis, based on early nadir mapping results taken near northern spring equinox, supported the conclusion that rapid stratospheric rotation is occurring (Flasar et al., 2005). More recently, a detailed analysis of zonal mean thermal structure and dynamics, based on CIRS data taken between July 2004 and September 2006, has been carried out by Achterberg et al. (2008). In the present work, we present an analysis of the longitudinal temperature structure based on CIRS nadir-viewing mapping data through May 2007. An offset of the stratospheric spin axis from the rotational axis of the solid body is found, and a possible explanation for this offset is proposed.

2. Data analysis

Atmospheric temperatures were obtained from nadir-viewing mapping sequences of thermal infrared spectra acquired with the Cassini orbiter Composite Infrared Spectrometer (CIRS). The instrument and its calibration are described in Flasar et al. (2004), and preliminary results are given in Flasar et al. (2005). For the observations used, the CIRS 1 by 10 mid-IR arrays (focal planes 3 and 4) were slewed across the observable hemisphere of Titan, producing maps with spatial resolution between 1.5° and 3° of great circle arc, covering the spectral range from 600 to 1400 cm^{-1} with an apodised spectra resolution of 2.8 cm^{-1}. Stratospheric tempera-

* Corresponding author at: NASA Goddard Space Flight Center, Code 693, Greenbelt, MD 20771, USA. Fax: +1 301 286 0212.
E-mail address: Richard.K.Achterberg@nasa.gov (R.K. Achterberg).

0019-1035/$ – see front matter
doi:10.1016/j.icarus.2008.05.014

Table 1
Summary of observations used for data analysis

Encounter	Start time	Duration	Mean longitude[a] (° west)	Mean latitude[a]	Mean resolution (° of arc)
T0	2004 Jul 02 03:30:21	13:30	356	38° S	2.1
Tb	2004 Dec 13 15:12:29	8:25	138	07° S	2.1
T3	2005 Feb 14 09:57:53	9:00	134	02° S	2.1
T3	2005 Feb 15 18:57:53	4:20	356	00° N	1.8
T4	2005 Apr 01 08:05:16	6:30	232	02° S	1.9
T6	2005 Aug 22 20:53:37	6:47	228	13° S	1.9
T8	2005 Oct 27 01:24:00	7:00	126	00° N	2.9
T8	2005 Oct 28 16:15:25	7:49	340	01° N	1.9
T9	2005 Dec 27 14:04:00	10:07	228	00° N	2.9
T10	2006 Jan 14 14:23:27	9:13	131	00° N	2.1
T14	2006 May 21 01:18:11	2:00	11	40° N	1.7
T14	2006 May 21 06:18:11	2:58	358	06° S	2.4
T15	2006 Jul 02 23:50:47	7:54	228	01° S	2.3
T17	2006 Sep 06 21:56:51	7:20	145	07° N	2.4
T18	2006 Sep 22 20:58:49	7:00	137	10° N	2.3
T19	2006 Oct 08 20:16:07	6:14	122	17° N	2.2
T21	2006 Dec 11 16:02:17	4:03	115	24° N	2.1
T22	2006 Dec 27 15:04:13	4:56	132	34° N	2.0
T23	2007 Jan 12 14:23:31	2:15	118	14° N	2.1
T23	2007 Jan 12 17:38:31	2:00	140	53° N	1.7
T23	2007 Jan 13 22:38:31	3:24	328	32° S	1.9
T24	2007 Jan 28 13:00:55	2:15	137	53° N	2.1
T24	2007 Jan 29 21:15:55	5:14	337	23° S	1.9
T26	2007 Mar 09 11:08:00	1:41	14	57° S	1.8
T27	2007 Mar 25 09:07:27	2:16	17	49° S	1.8
T28	2007 Apr 11 12:58:00	7:14	237	23° N	2.2
T30	2007 May 12 05:45:58	1:24	16	22° S	1.8
T30	2007 May 13 10:09:58	1:19	227	15° N	1.9

[a] Each map covers an circular area with a diameter of ∼120° of arc centered on the mean latitude and longitude.

tures were retrieved from individual spectra in the maps, using the ν_4 band of CH_4 between 1250 and 1311 cm^{-1}; the details of the retrieval process are discussed in Achterberg et al. (2008). The retrievals give temperature to an uncertainty of ∼0.5 K over the pressure range of approximately 0.2 to 5 mbar, with maximum information at 1 mbar (approximately 190 km above Titan's surface), except at high northern latitudes where the deep pressure limit decreases to ∼1 mbar. The data maps and their spatial coverage are summarized in Table 1. Collectively, the maps provide global coverage, but spread over an approximately three year period.

Analysis of the longitudinal thermal structure observed in these maps complements the study of the zonal mean structure by Achterberg et al. (2008). Although the time intervals between the various maps are too long for the study of high frequency waves or instabilities, stationary or slowly moving waves can be detected. Fig. 1A shows the temperature deviations from the zonal mean as a function of longitude for the data from all nadir maps in a 5° wide bin centered at 40° N. Despite the data covering a period of over three years, coherent longitudinal structure dominated by wavenumbers 1 and 2 is clearly visible. To see if a phase velocity can be estimated, a Lomb–Scargle periodogram (Press and Teukolsky, 1988) was calculated for a range of assumed phase velocities. Fig. 1B shows the resulting power as a function of the assumed wave frequency for the data in Fig. 1A, along with similar analyses for three other latitude bands. The maxima occur with westward phase speeds near 22.6°/day, which is very close to Titan's rotational frequency (22.5769768°/day), suggesting the possibility that the wave is diurnal. However, this is also close to the phase speed that would be observed if the wave were fixed in inertial space, and it is not possible to unambiguously distinguish between the two with the current data. Fig. 1C shows the same data after transformation into a Sun-fixed reference frame with the sub-solar point at 180° W longitude. A clear longitudinal structure, now close to a pure wavenumber 1, is still visible with somewhat less scatter about the fit than in the Titan-fixed reference frame.

Least-squares fits to the amplitude and phase for zonal wavenumber 1 as functions of latitude are shown in Fig. 2. The results in Figs. 2A and 2B are for a Sun-fixed reference frame. A comparison of the meridional structure of this wavenumber 1 feature with the zonal mean temperature field (Achterberg et al., 2008) shows that the wave amplitude is correlated with the meridional temperature gradient. The zonal-mean 1-mbar temperatures decrease toward both poles, although much more rapidly in the northern hemisphere. The wavenumber 1 amplitude is largest at the latitudes and altitudes where the meridional temperature gradient is largest, and the phase flips 180° near the equator where the meridional temperature gradient changes sign. This correlation and phase change would occur if the temperatures were zonally symmetric about an axis of rotation that was offset from Titan's pole. To check this, a function minimization algorithm (Nelder and Mead, 1965) was used to find the rotation axis offset that minimizes the global variance of the 1 mbar temperatures from their zonal mean. The amplitude and phase of zonal wavenumber 1 in the resulting tilted reference frame, with a rotation pole offset from the IAU definition of Titan's pole (Seidelmann et al., 2007) by 4.1°, is shown in Figs. 2C and 2D. Recent analysis of Cassini radar data (Stiles et al., 2008) shows the true spin pole to be about 0.3° different from the IAU pole, a correction unimportant for the present analysis. In the offset frame, the amplitude of wavenumber 1 has been greatly decreased, with amplitudes generally less than about 0.4 K, except at high northern latitudes where the maximum pressure to which the data are sensitive is decreasing. It therefore appears that the observed wavenumber 1 temperature feature can be explained by a temperature structure that is zonally symmetric about an axis that is offset from Titan's solid body pole direction by just over 4°. The azimuth of the thermal symmetry axis is about 76° west of the sub-solar longitude. If we instead assume that wavenumber 1 is stationary in an inertial frame, the azimuth of the symmetry axis is about 84° east of the sub-Saturn longitude at periapsis. Monte Carlo calculations give an uncertainty in the pole offset of 0.2°, and in the azimuth of 2°.

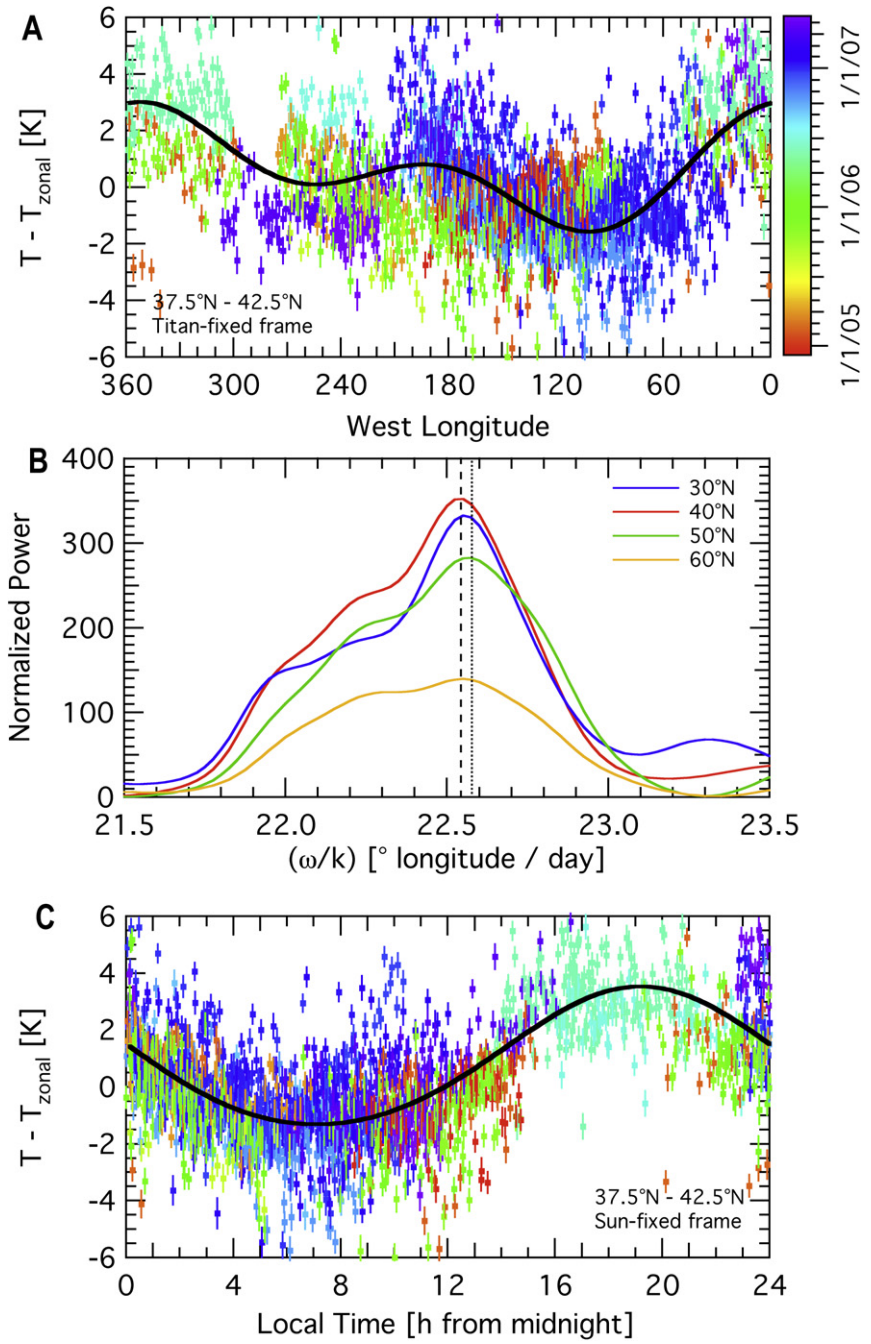

Fig. 1. (A) Temperature deviations from the zonal mean at the 1 mbar level as a function of longitude in a Titan-fixed reference frame. The temperatures were retrieved from CIRS spectra within a 5°-wide latitude band centered on 40° N. The data points are color coded according to the approximate date of acquisition with the scale shown to the right of the upper panel. The error bars represent the 1-sigma random error in the retrievals resulting from propagation of measurement noise. (B) Power as a function of assumed phase velocity obtained using a Lomb–Scargle periodogram analysis of the data shown in (A), along with similar analyses from three other latitude bands as indicated. The power has been normalized by the data variance. The range shown includes the phase speeds corresponding to a solar-fixed reference (vertical dashed line) and a reference fixed in inertial space (vertical dotted line). (C) The same data as (A), but in a solar-fixed reference frame. The solid line represents a least-squares fits to zonal wavenumbers 1 and 2.

We have performed fits for the tilt at other pressure levels, which suggest that the tilt gets smaller at higher pressures. However, poleward of 50° N, where we have the strongest temperature gradients which best constrain the fit for the axis tilt, we rapidly lose temperature information at pressures greater than 1 mbar (the cold lower stratosphere and warm upper stratosphere shift the weighting functions to lower pressures). Therefore, it is not clear if the apparent decrease in the tilt at higher pressures is real or an artifact of the information content of the data.

Since the north pole of Titan is now tilted away from the Sun, the thermal axis has smaller obliquity than Titan's spin axis, and the solar declination is reduced in the frame aligned with the thermal structure. Polar projection temperature maps for the 1 mbar atmospheric pressure level are shown in Fig. 3. The offset of the axis of symmetry of the thermal structure from Titan's axis of rotation is quite obvious in the northern (winter) hemisphere where the latitudinal temperature gradients are strong. Although present in the southern (summer) hemisphere, it is less obvious because of the relatively weak latitudinal temperature structure. Gradient

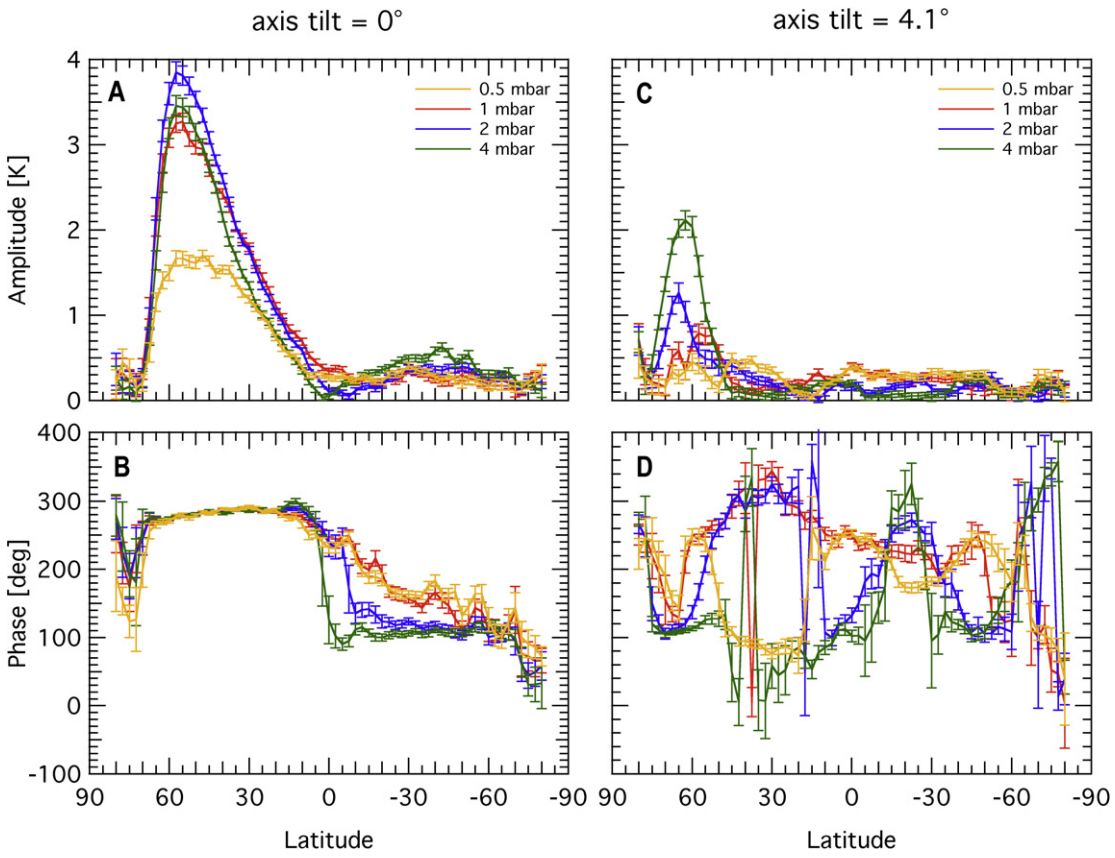

Fig. 2. Least-squares fit to the amplitudes (A) and phases (B) of zonal wavenumber 1 at the indicated pressure levels for a Sun-fixed reference frame aligned with Titan's solid-body rotation axis. A phase of 0 corresponds to warmest temperatures at the anti-solar longitude. Latitude bins of 5° were used. Analyses of the same data, but with the reference frame offset from Titan's axis by 4.1°, are shown in (C) and (D).

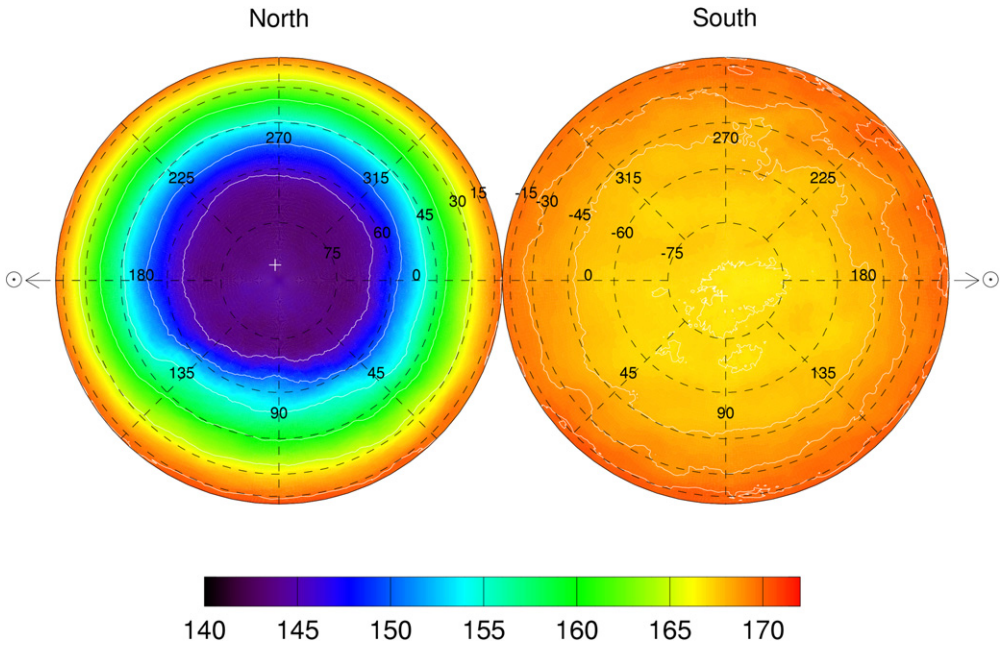

Fig. 3. Polar projection maps of retrieved temperatures at the 1 mbar level. The northern hemisphere is shown on the left and the southern hemisphere on the right. The color coded temperature scale in kelvins is shown at the bottom. The superposed grid represents latitude and west longitude in a Sun-fixed frame with the longitude of the sub-solar point at 180° W, such that the Sun direction is towards the left and right edges of the figure. Temperature contours are plotted at intervals of 5 K in the northern hemisphere, and 1 K in the southern hemisphere. The fitted axis of symmetry is indicated by a white cross (+).

thermal wind balance requires that the super-rotating stratospheric flow be parallel to the isotherms. This form of dynamical balance, within the context of Titan's atmosphere, has been previously discussed (Flasar et al., 2005; Achterberg et al., 2008).

3. Discussion

In principle, there are a number of mechanisms that can produce large-scale atmospheric wave structure. At first glance, the observed phase speed suggests that the wavenumber 1 feature may be tidal, but the gravitational tide is wavenumber 2, and cannot explain a wavenumber 1 feature. The solar diurnal tide does have a wavenumber 1 component. However, the thermal time constant in the mid-stratosphere is an order of magnitude longer than the Titan day (Flasar et al., 1981), and the wavenumber 1 response is strongest in the winter hemisphere where the solar forcing is weakest. It is thus unlikely that solar forcing is responsible for the observed response. Another possibility is a stationary wave induced by surface relief. A wavenumber 1 elevation amplitude of 20 m at the surface can produce a temperature amplitude of about 1 K at the 190 km or 1 mbar level, based on an assumed propagating wave with amplitude growing in height as $(p_0/p)^{1/2}$ where p_0 and p are pressure at the surface and at elevation, respectively. However, if surface topography excites the wave, the pattern should remain fixed in Titan coordinates, not fixed relative to the Sun or inertial space. It also seems unlikely that the phase of such a wave would be uniform in latitude, as the observations indicate, and it seems unlikely that the maximum amplitude would happen to fall at the same latitude as the winter midlatitude jet. A more probable explanation exists, under which these properties are not a coincidence.

Some of the theories that have been put forward to explain superrotation in planetary atmospheres rely on a meridional circulation with upward branch near the latitudes farthest from the rotation axis, in order to provide a net upward transport of angular momentum to balance downward frictional diffusive transport (Gierasch, 1975). Some of the general circulation model results for super-rotating atmospheres appear to be consistent with this theoretical concept (Del Genio and Suozzo, 1987; Hourdin et al., 1995, 2004). The mechanism is illustrated in Fig. 4. In the left panel, maximum integrated solar heating is assumed to occur away from the equator producing a meridional circulation unfavorable for the upward transport of zonal angular momentum. In the middle panel, the region of maximum solar heating is near the equator, and the resulting meridional circulation efficiently transports angular momentum upward to maintain a strong zonal flow with spin axis aligned with the solid body rotation axis. On Venus, the spin of the solid planet is close to perpendicular to the orbit plane, and a symmetric meridional circulation similar to that illustrated in the middle panel of Fig. 4 with rising branch at the equator satisfies both dynamical and heat redistribution requirements.

However, on a body such as Titan with the spin axis tilted relative to the perpendicular to the orbit plane, a flow might develop with an inclined spin axis that gives an excess of heating slightly offset from the spin equator while still maintaining sufficiently close alignment with the solid body rotation to be able to feed on its angular momentum. Strongly super-rotating planetary flows presumably require feedbacks between the mean flow, the heating distribution, and the momentum transports. By altering the spin axis of the flow relative to the solid body spin axis, the effective solar declination can be altered. A different heat distribution will then exist, because the flow averages day–night variations around a new set of latitude circles.

For a rotating sphere, the latitude of maximum diurnally averaged solar heating is farthest from the rotational equator for high solar declination. Since the rising branch of the mean meridional circulation is required to be far from the rotation axis in order to transport angular momentum upward, a high solar declination is unfavorable. Calculations of the diurnally integrated insolation, shown in Fig. 5, indicate that the solar declination must be less than approximately 30° in order to have the strongest solar heating near the equator. We propose that the Titan atmospheric spin, by feedbacks between the circulation and the heating, adjusts the flow to meet the constraint of low latitude heating with the atmospheric spin axis slightly offset from that of the solid satellite as implied by the observed thermal data.

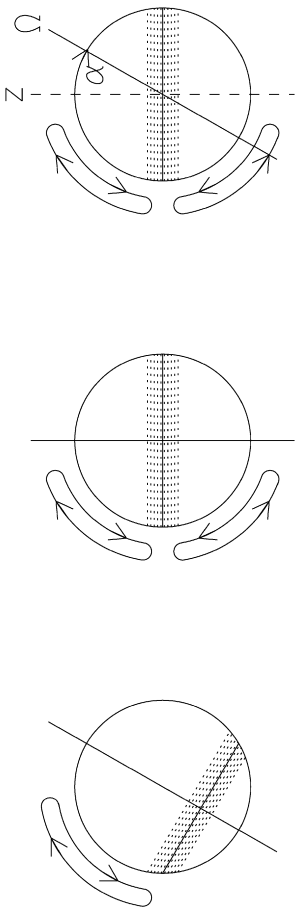

Fig. 4. Geometry of spin model. Schematic representations of possible meridional circulation patterns are displayed. The hatched areas represent regions of maximum integrated solar heating, assumed to be associated with the upwelling portions of the cells. In the case depicted on the left, the upward and downward branches of the cell are at similar distances from the rotation axis, and little upward net transport of angular momentum can occur. In contrast, the upward transport of angular momentum is maximized by the configuration shown in the middle panel. In the right-hand panel the meridional circulation axis (z) is shown vertical, and aligned with the perpendicular to the solar motion around the ecliptic.

We have investigated the proposed mechanism using a highly simplified model consisting of n atmospheric shells, each with thickness Δr. Each shell is assumed to be in rigid body rotation and subject to frictional interaction with its immediate neighbors, modeled as a linear drag proportional to the difference in angular velocity between shells. This is analogous to a vertical eddy viscosity. The frictional interaction between the lower surface of the bottom shell and the solid satellite surface permits angular momentum exchange between the atmosphere and the solid body. Angular momentum is advected by an imposed vertical velocity field, which is assumed to be independent of height except at the top of the upper shell and the bottom of the lowest shell where it vanishes. We offer as a hypothesis that while a tilt of the meridional circulation may not be necessary to produce superrotation, it will enhance it.

The latitude dependence of the vertical velocity is arbitrarily chosen to be proportional to a second order Legendre polynomial, with sign chosen to ensure that upward motion occurs at the "equator" of the meridional circulation. The amplitude is con-

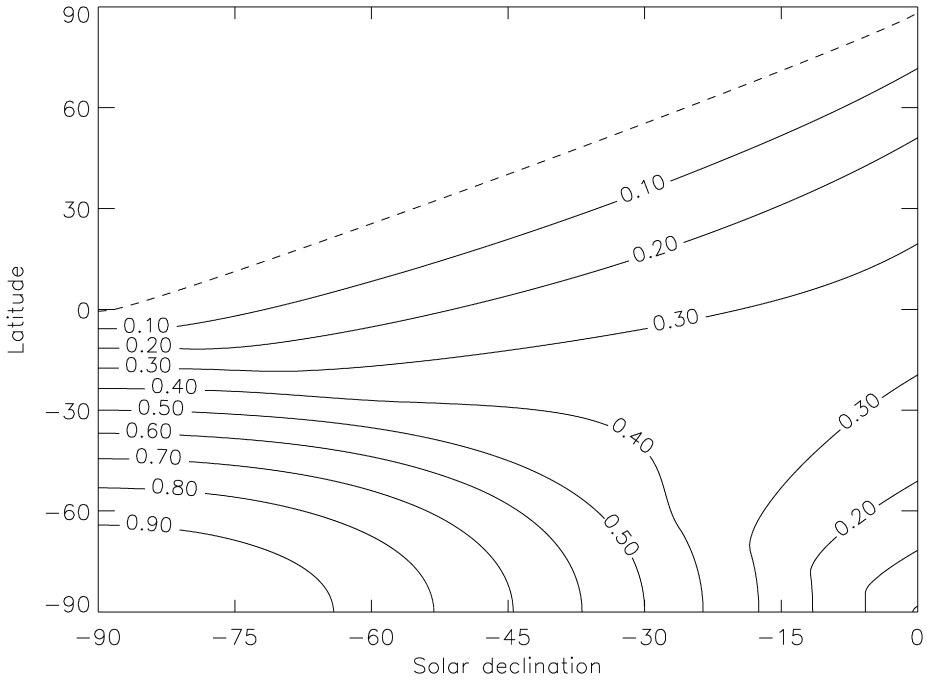

Fig. 5. Insolation as function of solar declination. A rapidly rotating atmosphere carries heat to the night side and leads to a heating distribution that depends on the solar declination in the rotating atmosphere frame. The declination must be less than about 30° to produce a heating maximum that is near the equator.

trolled by a coefficient W, one of the parameters of the model. The z-axis of the coordinate system is chosen as the axis of symmetry or "pole" of the circulation, and the solid body angular velocity vector $\mathbf{\Omega}$ is assumed to be at an angle α to this axis. As discussed above, α should be less than 30° or so to efficiently pump angular momentum upward. Alpha depends on the declination of the Sun in a frame rotating with the atmosphere. The meridional circulation, in passing from shell to shell, carries with it the angular momentum representative of its shell of origin. The rate of deposition of angular momentum into a shell by vertical advection is obtained by calculating the difference between the angular momentum flux integrated over the lower surface of the shell and that integrated over the upper surface. These considerations result in a set of equations for the time rate of change of the angular velocities $\boldsymbol{\omega}_i$ $(i = 1, \ldots, n)$ of the n shells.

A frictional time constant is defined as $t_F = H^2/K$ where K is a vertical eddy viscosity coefficient and $H = n\Delta r$ is the total atmospheric depth. The dynamic time constant is $t_D = H/W$. The ratio of these time constants is a parameter of the model, with the most rapid spin corresponding to $0 < t_D/t_F < 1$. The model is a straightforward extension of that used by Gierasch (1975), modified to permit an angular offset between the meridional circulation axis of symmetry and the planetary spin. When the amplitude W is positive and the number of shells is large, the angular velocity of the shells increases exponentially with height. Examples of steady state solutions obtained for a 2-shell model are given in Fig. 6 for a range of values of t_D/t_F. The magnitude of the angular velocity of the top shell shows maximum superrotation in all cases when the axis of symmetry of the meridional circulation is coincident with the solid body rotation axis ($\alpha = 0$), the configuration most favorable for angular momentum exchange with the solid body. This is consistent with the recent general circulation model results of Yamamoto and Takahashi (2007). In all cases, the direction of the top layer spin lies between the direction of the solid body spin $\mathbf{\Omega}$ and the direction of the meridional circulation axis, as shown in Fig. 6. The simple model responds to changes in forcing with a time lag, consistent with the observation that the spin pole currently lags behind the direction toward the Sun. The time constants t_D and t_F are much longer than the diurnal period but may be shorter than the seasonal time. Presumably they are related to the radiative-dynamical response time of the atmosphere, whose determination can be complicated (Flasar and Conrath, 1990). Annually, the atmospheric spin is expected to precess about an axis normal to the plane of Saturn's orbit, as the spin seeks alignment of the spin equator with the direction toward the Sun. More complete modeling must include feedback between the atmospheric spin and the meridional circulation, along with its relationship to the integrated solar heating. However, this simple model illustrates the tendency for the atmospheric spin to seek a compromise orientation when the meridional circulation axis and the planetary spin axis are not aligned. The compromise orientation permits both adequate vertical angular momentum transport and efficient extraction of angular momentum from the solid body.

General circulation experiments with seasonally varying heating have been carried out (Hourdin et al., 2004; Tokano et al., 1999; Yamamoto and Takahashi, 2007; Richardson et al., 2007) but published reports of results have not presented diagnostics of the atmospheric spin direction at different heights. At present the new observation reported here cannot be easily compared with numerical models. This is clearly an objective for future modeling experiments.

The observational test of this conjecture by tracking the atmospheric spin orientation will require seasonal monitoring of the circulation pattern. At least one quarter of a Titan year, or about 7 Earth years, should be observed. Another possible observational objective would be the configuration of the meridional circulation and its changes over time. But the circulation in the forcing region near and below the base of the stratosphere is the most important, and is difficult to obtain.

Acknowledgment

This work has been supported by the NASA Cassini Project.

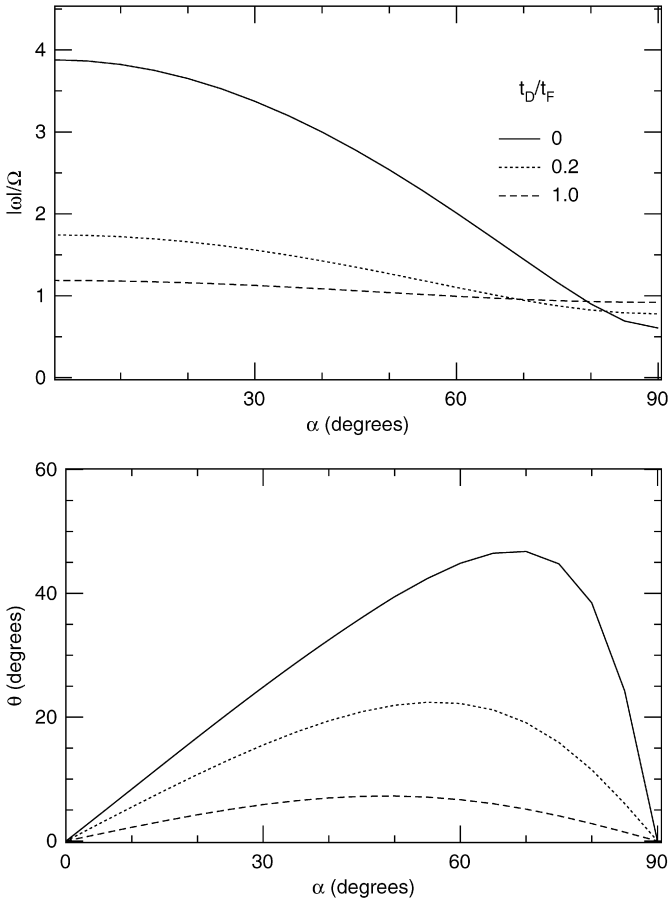

Fig. 6. (Top) Magnitude of the angular velocity of the top shell of a 2-shell model divided by the magnitude of the solid body angular velocity as a function of α, the angle between the axis of symmetry of the imposed meridional circulation and the solid body spin vector. Results are given for a range of values of the ratio of the dynamic time scale to the frictional time constant, t_D/t_F. (Bottom) The angle θ between the spin vector of the top shell and the solid body rotation vector as a function of α, the angle between the axis of symmetry of the meridional circulation and the solid-body rotation axis.

References

Achterberg, R.K., Conrath, B.J., Gierasch, P.J., Flasar, F.M., Nixon, C.A., 2008. Titan's middle-atmospheric temperatures and dynamics observed by the Cassini Composite Infrared Spectrometer. Icarus 194, 263–277.

Bouchez, A.H., 2003. Seasonal trends in Titan's atmosphere: Haze, wind, and clouds. Ph.D. thesis, California Institute of Technology, URL: http://resolver.caltech.edu/CaltechEDT:etd-10272003-092206.

Del Genio, A.D., Suozzo, R.J., 1987. A comparative study of rapidly and slowly rotating dynamical regimes in a terrestrial general circulation model. J. Atmos. Sci. 44, 973–986.

Fast, K.E., Kostiuk, T., Espenak, F., Buhl, D., Livengood, T.A., Goldstein, J., 1994. Direct measurement of Doppler shifts due to zonal winds on Titan. Bull. Am. Astron. Soc. 26, 1183.

Flasar, F.M., Conrath, B.J., 1990. Titan's stratospheric temperatures—A case for dynamical inertia? Icarus 85, 346–354.

Flasar, F.M., Samuelson, R.E., Conrath, B.J., 1981. Titan's atmosphere—Temperature and dynamics. Nature 292, 693–698.

Flasar, F.M., Kunde, V.G., Abbas, M.M., Achterberg, R.K., Ade, P., Barucci, A., B'ezard, B., Bjoraker, G.L., Brasunas, J.C., Calcutt, S., Carlson, R., C'esarsky, C.J., Conrath, B.J., Coradini, A., Courtin, R., Coustenis, A., Edberg, S., Edgington, S., Ferrari, C., Fouchet, T., Gautier, D., Gierasch, P.J., Grossman, K., Irwin, P., Jennings, D.E., Lellouch, E., Mamoutkine, A.A., Marten, A., Meyer, J.P., Nixon, C.A., Orton, G.S., Owen, T.C., Pearl, J.C., Prang'e, R., Raulin, F., Read, P.L., Romani, P.N., Samuelson, R.E., Segura, M.E., Showalter, M.R., Simon-Miller, A.A., Smith, M.D., Spencer, J.R., Spilker, L.J., Taylor, F.W., 2004. Exploring the Saturn system in the thermal infrared: The Composite Infrared Spectrometer. Space Sci. Rev. 115, 169–297.

Flasar, F.M., Achterberg, R.K., Conrath, B.J., Gierasch, P.J., Kunde, V.G., Nixon, C.A., Bjoraker, G.L., Jennings, D.E., Romani, P.N., Simon-Miller, A.A., Bézard, B., Coustenis, A., Irwin, P.G.J., Teanby, N.A., Brasunas, J., Pearl, J.C., Segura, M.E., Carlson, R.C., Mamoutkine, A., Schinder, P.J., Barucci, A., Courtin, R., Fouchet, T., Gautier, D., Lellouch, E., Marten, A., Prangé, R., Vinatier, S., Strobel, D.F., Calcutt, S.B., Read, P.L., Taylor, F.W., Bowles, N., Samuelson, R.E., Orton, G.S., Spilker, L.J., Owen, T.C., Spencer, J.R., Showalter, M.R., Ferrari, C., Abbas, M.M., Raulin, F., Edgington, S., Ade, P., Wishnow, E.H., 2005. Titan's atmospheric temperatures, winds, and composition. Science 308, 975–978.

Gierasch, P.J., 1975. Meridional circulation and the maintenance of the Venus atmospheric rotation. J. Atmos. Sci. 32, 1038–1044.

Hourdin, F., Talagrand, O., Sadourny, R., Courtin, R., Gautier, D., McKay, C., 1995. Numerical simulation of the general circulation of the atmosphere of Titan. Icarus 117, 358–374.

Hourdin, F., Lebonnois, S., Luz, D., Rannou, P., 2004. Titan's stratospheric composition driven by condensation and dynamics. J. Geophys. Res. 109. E12005.

Hubbard, W.B., Sicardy, B., Miles, R., Hollis, A.J., Forrest, R.W., Nicolson, I.K.M., Appleby, G., Beisker, W., Bittner, C., Bode, H.-J., Bruns, M., Denzau, H., Nezel, M., Riedel, E., Struckmann, H., Arlot, J.E., Roques, F., Sevre, F., Thuillot, W., Hoffmann, M., Geyer, E.H., Buil, C., Colas, F., Lecacheux, J., Klotz, A., Thouvenot, E., Vidal, J.L., Carreira, E., Rossi, F., Blanco, C., Cristaldi, S., Nevo, Y., Reitsema, H.J., Brosch, N., Cernis, K., Zdanavicius, K., Wasserman, L.H., Hunten, D.M., Gautier, D., Lellouch, E., Yelle, R.V., Rizk, B., Flasar, F.M., Porco, C.C., Toublanc, D., Corugedo, G., 1993. The occultation of 28 SGR by Titan. Astron. Astrophys. 269, 541–563.

Kostiuk, T., Fast, K.E., Livengood, T.A., Hewagama, T., Goldstein, J.J., Espenak, F., Buhl, D., 2001. Direct measurement of winds of Titan. Geophys. Res. Lett. 28, 2361–2364.

Kostiuk, T., Livengood, T.A., Hewagama, T., Sonnabend, G., Fast, K.E., Murakawa, K., Tokunaga, A.T., Annen, J., Buhl, D., Schmülling, F., 2005. Titan's stratospheric zonal wind, temperature, and ethane abundance a year prior to Huygens insertion. Geophys. Res. Lett. 32, doi:10.1029/2005GL023897. L22205.

Nelder, J.A., Mead, R., 1965. A Simplex-method for function minimization. Comput. J. 7, 308–313.

Press, W.H., Teukolsky, S.A., 1988. Search algorithm for weak periodic signals in unevenly spaced data. Comput. Phys. 2, 77–82.

Richardson, M.I., Toigo, A.D., Newman, C.E., 2007. PlanetWRF: A general purpose, local to global numerical model for planetary atmospheric and climate dynamics. J. Geophys. Res. 112. E09001.

Seidelmann, P.K., Archinal, B.A., A'Hearn, M.F., Conrad, A., Consolmagno, G.J., Hestroffer, D., Hilton, J.L., Krasinsky, G.A., Neumann, G., Oberst, J., Stooke, P., Tedesco, E.F., Tholen, D.J., Thomas, P.C., Williams, I.P., 2007. Report of the IAU/IAG Working Group on cartographic coordinates and rotational elements. Celest. Mech. Dynam. Astron. 98, 155–180.

Sicardy, B., Ferri, F., Roques, F., Lecacheux, J., Pau, S., Brosch, N., Nevo, Y., Hubbard, W.B., Reitsema, H.J., Blanco, C., Carreira, E., Beisker, W., Bittner, C., Bode, H.-J., Bruns, M., Denzau, H., Nezel, M., Riedel, E., Struckmann, H., Appleby, G., Forrest, R.W., Nicolson, I.K.M., Hollis, A.J., Miles, R., 1999. The structure of Titan's stratosphere from the 28 Sgr occultation. Icarus 142, 357–390.

Stiles, B.W., Kirk, R.L., Lorenz, R.D., Hensey, S., Lee, E., Ostro, S.J., Allison, M.D., Callahan, P.S., Yonggyu, G., Iess, L., del Marmo, P.P., Hamilton, G., Johnson, W.T.K., West, R.D., and the Cassini Radar Team, 2008. Determining Titan's spin state from Cassini radar images. Astron. J. 135, 1669–1680.

Tokano, T., Neubauer, F.M., Laube, M., McKay, C.P., 1999. Seasonal variation of Titan's atmospheric structure simulated by a general circulation model. Planet. Space Sci. 47, 493–520.

Yamamoto, M., Takahashi, M., 2007. A parametric study of atmospheric superrotation on Venus-like planets: Effects of oblique angle of planetary rotation axis. Geophys. Res. Lett. 34. L16202.